ChemSusChem

Research Article
doi.org/10.1002/cssc.202300486

Chemistry Europe
European Chemical Societies Publishing

www.chemsuschem.org

Reconsidering Anode Materials for Fluoride-Ion Batteries– The Unexpected Roles of Carbide Formation**

Don McTaggart,[a] Scott C. Warren,*[a] and Oliver Clemens*[b]

Carbon is a ubiquitous additive to enhance the electrical conductivity of battery electrodes. Although carbon is generally assumed to be inert, the poor reversibility seen in some fluoride-ion battery electrodes has not been explained or systematically explored. Here, we utilize the Materials Project database to assess electrode deactivation reactions that result in the formation of a metal carbide. Specifically, we compare the theoretical potentials of MF_y reduction to either the corresponding metal M or metal carbide MC_x. We find that the formation of MC_x is unlikely to be important in anodes that operate at modest reduction potentials, such as those made from electronegative metals like Zn, Sn, or Pb. However, in anodes that operate at extreme reduction potentials, such as alkaline earths or lanthanides, we find that formation of MC_x is relevant and can emerge as a mechanism for capacity loss. Thus, side reactions of metals with carbon additives that form metal carbides possibly explain the poor reversibility of lanthanide or alkaline earth metal-based electrode materials. Finally, we highlight that the carbide formation process might be exploited for designing cheap anode systems with improved reversibility.

Introduction

The growing reliance on renewable energy and the increasing demands of grid storage, electric vehicles, and portable electronics necessitates the development of battery technologies beyond lithium-ion batteries (LIBs). Although LIBs offer excellent performance, the limited availability of certain critical elements, such as Co and Li,[1] has led to an increased focus on alternative types of batteries, which could offer longer-lasting and more sustainable supply chains. One possible alternative is the fluoride-ion battery (FIB),[2] which uses fluoride ions (F^-) as the ionic charge carrier instead of Li^+.

Although investigations of fluoride-ion conductors have been performed for many years,[3] serious consideration of FIB technology only began to emerge after the recent proof-of-concept demonstration by Reddy and Fichtner.[2a] In this work, they used $La_{0.9}Ba_{0.1}F_{2.9}$ as a solid electrolyte in combination with composite conversion-type electrode materials $MF_y + M$, where the latter converts between the metal state M and the metal fluoride state MF_y within the electrochemical reaction. Since this initial demonstration, a wider range of electrolytes and electrodes have been explored. This has included liquid and polymer electrolytes[4] as well as intercalation-based electrodes.[5] Despite this progress, challenges with electrode stability are often observed.

Almost universally, FIB electrodes contain a carbon-based conductive additive (e.g., acetylene black, carbon black, or carbon nanotubes). Although carbon is typically considered an inert additive, recent work uncovered the unexpected oxidation of carbon, as identified via XPS measurements that showed the shift in carbon to higher binding energies.[5f] Unwanted side reactions can also be observed under reducing conditions. Wissel et al.[6] studied the electrochemical topochemical reduction of $La_2NiO_3F_2$[7] within a solid-state FIB, attempting to form partially defluorinated $La_2NiO_3F_{1.93}$ and La_2NiO_3F, both of which require reduction of Ni^{2+} to Ni^+. Remarkably, they observed only the formation of $La_2NiO_3F_{1.93}$, even though the charging plateau exceeded the theoretical capacity for forming La_2NiO_3F by a factor of four. XPS revealed that this additional capacity was accompanied by a shift in carbon to lower binding energies, suggesting that the carbon black was becoming reduced. Due to the absence of other reactants, it is likely that this reduction might result from the interaction with the metals contained within the active material and additives in contact with carbon.

A possible reduction pathway for elemental carbon involves cation intercalation. As a common example, Li inserts into graphitic carbon to form LiC_6, the desired anode reaction for LIBs. Alternatively, if the carbon lacks a layered structure, a metal carbide may result. In fact, because a carbide can have a formal oxidation state of -IV, pure carbon has a theoretical capacity of 8934 $mAh\,g^{-1}$. Although this capacity is purely hypothetical, conventional batteries often contain 10–25 wt%

[a] D. McTaggart, Prof. Dr. S. C. Warren
Department of Chemistry, Kenan Lab A808
University of North Carolina at Chapel Hill
Chapel Hill, NC 27514-3290 (United States of America)
E-mail: sw@unc.edu
Homepage: http://materials-lab.io
[b] Prof. Dr. O. Clemens
Institute for Materials Science, Materials Synthesis Group
University of Stuttgart
Heisenbergstraße 3, 70569 Stuttgart (Germany)
E-mail: oliver.clemens@imw.uni-stuttgart.de
Homepage: http://www.imw.uni-stuttgart.de/mc

[**] A previous version of this manuscript has been deposited on a preprint server (10.26434/chemrxiv-2022-fww5l)

Supporting information for this article is available on the WWW under https://doi.org/10.1002/cssc.202300486

carbon. Therefore, even as an additive, the capacity of carbon could exceed that of the active materials, consistent with the earlier findings.[6]

Despite this evidence, side-reactions in FIB anodes have not been previously considered. Therefore, in this work, we compare two possible anode reduction reactions that can occur by reducing a metal fluoride in the presence of carbon additives. The first is the reduction of the metal fluoride to metal; the second is the reduction of the carbon to form a metal carbide. We investigate the competing energetics of these reactions by comparing the formation energies for all elemental metals within the Materials Project database[8] that are known to exist as both a metal fluoride and a metal carbide. From these results, we identify periodic trends and derive guidelines for the choice of electron conducting additives in fluoride-ion batteries.

Results and Discussions

Metal carbides in the context of fluoride-ion batteries (FIBs)

A typical anode composite in the discharged state normally consists of a metal fluoride MF_y, a carbon additive, and a fluoride conductor, which would be a second metal fluoride in the case of all solid-state FIBs. These materials are often intimately ground together, for example, via planetary ball milling, to keep particle sizes small to facilitate the transformation process. During the reduction process of the anode material, i.e., charging, one can consider two reactions that are in competition with each other.

$$MF_y + y\ e^- + x\ C \rightarrow M + y\ F^- + x\ C \quad (1)$$

$$MF_y + y\ e^- + x\ C \rightarrow MC_x + y\ F^- \quad (2)$$

These reactions differ with respect to the chemical species that is being reduced. For Equation (1), the reduction occurs on the metal directly, whereas for Equation (2), the reduction occurs at the carbon and/or at the metal, depending on the difference in the electronegativities of M and C.

Equation (1) is a common conversion reaction of a metal fluoride to a metal. Its chemical and therefore electrochemical potential depends on the reductivity of the metal, represented by the Fermi energy of the metal, as well as the lattice energies of both the metal M and the metal fluoride MF_y. We acknowledge that practically, the MF_y compound with the lowest value of y is most relevant to be used as an anode material (although all MF_y compounds within 0.075 eV/atom of the hull were included in our considerations). To illustrate this, one can compare the potentials of FeF_2/FeF_3 and Fe/Fe_3, as a representative for MF_y/MF_{y+1} and M/MF_{y+1}. For example, before FeF_3 (total energy: −6.19 eV/atom) is reduced to metallic Fe, reduction to FeF_2 (total energy: −6.69 eV/atom) occurs at a potential of ≈ 0.8 V higher than the potential of Fe/FeF_3.

Equation (2) is a complex reaction. To understand the potential impact of the kinetics of carbide formation, the microscopic structure becomes important. Thus, we first discuss the structure of carbon blacks as a representative additive.[9] Carbon blacks can have different degrees of crystallinity or amounts of defects, depending on the synthesis conditions that have been used for material preparation. They can be obtained from the pyrolysis of hydrocarbons and consist of regions in which sp^2 hybridized carbon layers are parallel to each other (graphite-related orientation), as well as disordered regions, even with sp^3-type or sp-type bonding. Metal insertion into the graphitic regions, similar to the lithiation of graphite, is a multistep process that occurs via staged filling of the graphitic layers. This insertion process requires a small degree of structural reorganization with mainly expansion along the c-axis but has a limited capacity per carbon atom (e.g., MC_6, see Figure 1a for structural depiction). For this process, the electrons are transferred to the empty states immediately above the Fermi level of graphite[10] (see Figure 1b). The insertion of metals has been reported not only for lithium[11] and potassium[12] but also for lanthanides (e.g., Yb and Eu) under the formation of metal inserted compounds.[13] These materials can be prepared by heating carbon under a metal vapor for volatile lanthanides or by heating compacted powders of carbon and metal.[13]

Metal insertion into graphite might likely be favourable for kinetic reasons, and for certain metals, such carbides also represent the thermodynamically most stable product (e.g.,

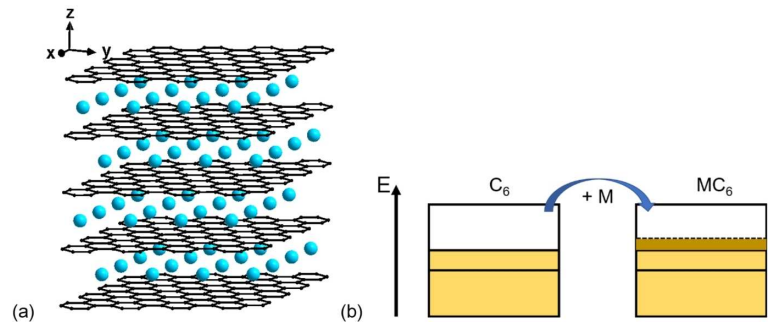

Figure 1. (a) Crystal structure of metal inserted graphite on the example of EuC_6. (b) Schematic depiction of the change in the electronic structure for M insertion into graphite.

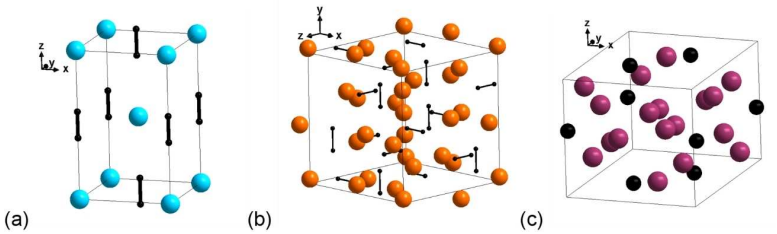

Figure 2. Crystal structures of EuC_2 (a), La_2C_3 (b), and Fe_3C (c).

EuC_6). However, carbon materials can also consist of regions with structures not related to graphite. For such regions, removal of carbide species under the formation of metal carbides (or nanoscopic clusters) might also be imagined, as well as the formation of surface adducts of the cationic metal species in addition to reduction of the host structure. Thus, it will also be important to consider carbide compounds such as EuC_2[14] (see Figure 2a) or La_2C_3[15] (see Figure 2b), which might represent the energetics of the metal cation to negatively charged carbon bonds. Similar considerations can be made for metal carbides with lower degree of ionic M–C bonding, for example, Fe_3C[16] (see Figure 2c).

In the following, we will discuss the energetics of both reactions (also see scheme shown in Figure 3). Lithium is a strong reductant forming highly stable LiF and will be used as the reference for the electrochemical potentials in this work. For reacting metal fluorides with lithium, all compounds are solid; thus, one can easily conclude that these reactions must be exothermal reactions with $\Delta H_1 < 0$ eV for metals which are solid at ambient temperature. The same holds true for the carbide formation of stable metal carbides (which cannot decompose into the elements), which will also be an exothermal reaction with $\Delta H_{carb.form.} < 0$ eV. Consequently, the enthalpy of the carbon reduction coupled to metallization from MF_y decomposition will be even more exothermal with $\Delta H_2 = \Delta H_1 + \Delta H_{carb.form.} < 0$ eV if a stable metal carbide exists. At this stage, we acknowledge that this is not true for all known carbides. Certain metal carbides (e.g., those of Au, Ag, and Hg) are prepared at temperatures above the melting point of the metal or via a gas phase reaction,[17] and their formation is only stabilized from overcoming the lattice energy of the metal, resulting in $\Delta H_{carb.form.} > 0$ eV.

Neglecting entropic contributions to the free enthalpy ΔG will automatically imply that the potential $U = \frac{-\Delta G}{zF} \approx \frac{-\Delta H}{zF}$ (with z being the number of transferred electrons and F being Faraday's constant; 96,485 C mol^{-1}) can be derived from the energy difference of products and reactants or from the differences of the reaction enthalpies of Equations (1) and (2), respectively, according to Equation (3) and Equation (4).

$$U(\mathrm{M/MF}_y)_{\text{vs. Li/LiF}} = -\frac{E(\mathrm{M}) + yE(\mathrm{LiF}) - yE(\mathrm{Li}) - E(\mathrm{MF}_y)}{y} = -\frac{\Delta H_1}{y\mathrm{F}} \quad (3)$$

$$U(\mathrm{MC}_x/\mathrm{MF}_y + x\mathrm{C})_{\text{vs. Li/LiF}} = -\frac{E(\mathrm{MC}_x) + yE(\mathrm{LiF}) - xE(\mathrm{C}) - yE(\mathrm{Li}) - E(\mathrm{MF}_y)}{y} = -\frac{\Delta H_2}{y\mathrm{F}} \quad (4)$$

Furthermore, one can consider the potential difference ΔU between carbon reduction and metal fluoride reduction, according to Equation (5).

$$\Delta U(\mathrm{MC}_x - \mathrm{M}) = U(\mathrm{MC}_x/\mathrm{MF}_y + x\mathrm{C})_{\text{vs. Li/LiF}} - U(\mathrm{M/MF}_y)_{\text{vs. Li/LiF}} = -\frac{E(\mathrm{MC}_x) + E(\mathrm{M}) - xE(\mathrm{C})}{y} = -\frac{\Delta H_2 - \Delta H_1}{y\mathrm{F}} = -\frac{\Delta H_{carb.form.}}{y\mathrm{F}} \quad (5)$$

From this, we conclude the following:

(1) The carbon reduction under metal carbide formation will become thermodynamically favourable over the metal fluoride reduction (i.e., the potential of the metallization-induced carbon reduction is higher than the potential of the metal fluoride reduction) for exothermal carbide formation reactions between carbon and metal fluoride. In these cases, the potential of $U(MC_x/MF_y + xC)$ will be higher than the potential of $U(M/MF_y)$, i.e., carbon would be a stronger oxidizer than the metal fluoride.

(2) The absolute value of this potential difference is proportional to $1/y$. Thus, the lower the metal-to-fluoride ratio in the MF_y compound, the higher will be $|\Delta U|$. If one considers a pair of metal fluorides MF_m and MF_n of the same metal M with $m < n$, this implies that the fluoride-poor

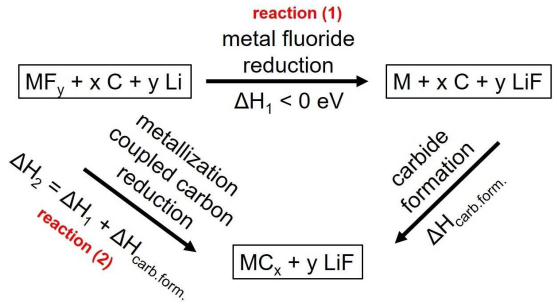

Figure 3. Reaction scheme comparing the energetics comparing the metal fluoride reduction [Eq. (1)], to the metallization coupled carbon reduction, [Eq. (2)].

metal fluorides can strongly favour metal carbide formation if $\Delta H_{carb.form.} < 0$ eV. In reality, overpotentials might affect the carbide formation process, and it is reasonable to assume that carbide materials with a structure close to graphite (respectively metal-poor carbides) might be favoured for kinetic reasons. This can become especially relevant if metals can form various MC_x metal carbides with different values of x, and some of them have more complex structures which require a strong degree of reorganization. From this one could in principle expect that the formation of a crystalline carbide induces strong overpotentials, which can then favour the metal fluoride reduction (see scheme in Figure 4a).

(3) Graphite is the thermodynamically most stable modification of carbon. The formation energy of metal carbides from metastable carbon species (e.g., non-graphitic regions within carbon materials) will thus be energetically more favourable and would lead to higher values of ΔU accordingly. We exemplified this by calculating the values of $U(MC_x/MF_{y+}{}^{x}/_{60}\,C_{60})$ and the corresponding ΔU values additionally. Though the absolute potential differences have to be read with caution, this shows that the formation of crystalline metal carbides would become energetically even more accessible (see Figure S1).

(4) Further, non-graphitic carbon can also form non-crystalline surface adducts of metals undergoing reduction. The energy of such metal carbides cannot be easily calculated and would require detailed DFT-based optimization which is beyond the scope of this manuscript. However, one can estimate the potential influence from the analogy of metals (e.g., Na) that do not form a stable carbide. For Na-ion batteries, it is known that although Na cannot be inserted into graphite, it can reduce non-graphitic carbon regions and form surface adducts there. This can happen at potentials just above the potential of Na/Na^+ (adsorption within micropores) up to ≈1–2 V for hard carbon materials and can be relevant for the commonly used carbon additives.

(5) Let us additionally consider the case of a metal carbide with an energy above the convex hull, i.e., being metastable under ambient conditions. From a simple energetic viewpoint, the corresponding metal fluorides should be transformed first to the metal in the reduction in the conversion process, followed by the reduction of carbon under the formation of the carbide. Practically, conversion processes are often accompanied by overpotentials, and the crystallization of the metal species to the thermodynamically most stable metallic state might be stronger impeded for kinetic reasons than the metal carbide formation itself (especially considering the non-graphitic regions within carbon materials and the formation of surface adducts). It has been discussed previously that this might be strongly impacted by the melting point of the metal and the fluoride ion conductivity of the corresponding metal fluoride.[18] Thus, if there are considerable overpotentials hindering the metal-to-metal fluoride transformation, carbide formation could in principle take place if it is itself not affected by similarly strong kinetic inhibition (see Figure 4b).

The values for $U(M/MF_y)_{vs.\ Li/LiF}$, $U(MC_x/MF_y + xC)_{vs.\ Li/LiF}$, and $\Delta U(MC_x - M)$ were calculated for all combinations of MF_y and MC_x available within the Materials Project Database. These values for the different potentials are tabulated in Table S1 and comprise the data for unstable metal carbides with energies above the convex hull. According to the considerations mentioned above, one can narrow these data by comparing the most reasonably stable MF_y compounds with the most stable metal carbides MC_x, which is graphically represented in Figure 5. This summary reveals valuable information about which elements might favour carbide formation prior to the reduction of the respective metal fluoride or when carbon interactions of the metal (not be confused with carbon fluorination for high voltage cathodes) might become relevant (limitations of the contained data are discussed at the end of this section).

These findings are summarized as follows:

(1) For the late first-row transition metals starting with Cu, as well as the late second/third-row transition metals starting with Ru and Os, respectively, metal formation seems to be

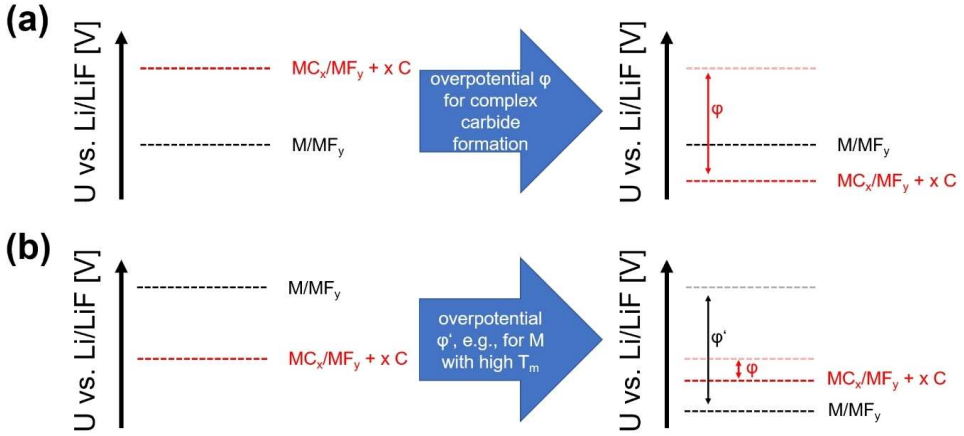

Figure 4. Schematic presentation of how overpotentials can help favour metal formation (a) or metal carbide formation (b) over the concurrent reaction.

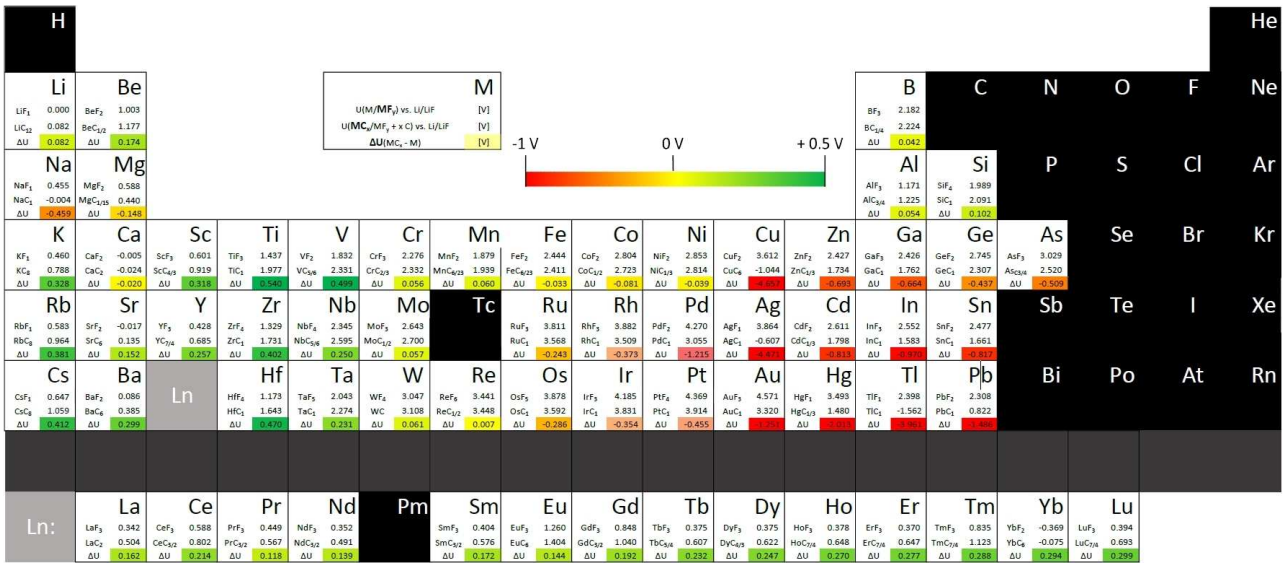

Figure 5. Comparison of $U(M/MF_y)_{vs.\ Li/LiF}$, $U(MC_x/MF_y + xC)_{vs.\ Li/LiF}$, and $\Delta U(MC_x - M)$ for the different combinations of stable MF_y with a low value of y and the thermodynamically most stable carbide MC_x. Actinides were not considered for the calculations since they do not show practical relevance. Furthermore, certain elements (Tc, Pm, Pb, Sb, Bi, Te, Po) did not contain any entries for their corresponding metal carbides. Furthermore, some elements form molecular carbides (H, N, O, S, Cl, Br, I) or do not form carbides at all (noble gases) and were thus not included.

the most plausible process for metal fluoride reduction. In addition, these M/MF_y combinations have high potentials, implying that these metals are likely to be used on the cathode side, for which the low potentials required for carbon reduction will be practically not induced. Indeed, for such materials one would rather expect an oxidation of carbon under formation of fluorinated carbon species as has been found for cathode materials.[5f] The unfavorability of carbide formation is further extended to the p-block metals of the respective row of the periodic table. Apart from Cu (which does not seem to form a reasonably stable carbide), all these metals form metal-rich carbides with $x \leq 1$. Considering that carbide formation would have to occur at the interface between M and C, this would imply that a fairly large metal cluster would have to form prior to the reaction with C. This consideration is of special importance for ZnF_2, PbF_2, or SnF_2, which have been recently investigated as reference electrodes or as anodes for FIBs.[5f,18–19] The values of $\Delta U(MC_x - M)$ for these metals are below −0.5 V, which renders the carbide formation energetically unfavourable and could explain why these materials appear to show good reversibility in FIBs. The fairly low melting points of these metals further supports the ease of the MF_y to M conversion process.

(2) Alkaline earth metals (apart from Na, Mg, Ca) form stable metal carbides and have potentials that are sufficiently low for them to be considered as anode materials within FIBs. Therefore, the corresponding metal fluorides are likely not to work as conversion materials in the presence of carbon since carbon reduction will be the most favourable process. Furthermore, we note that all these metals form carbon-rich carbides with $x \gg 1$; the corresponding structures are graphite-related, with metal ions inserted between the graphene layers. Considering that metal insertion into graphite is a process that requires fairly low structural reorganization and thus potentially low thermal activation, we conclude that carbide formation will likely dominate over metal formation for most alkaline and alkaline earth metals. This consideration will become particularly important when using anodes such as SrF_2, BaF_2, or tysonite-/fluorite type solid fluoride ion conductors.[19a,20] However, the impacts of carbide formation might not be entirely negative, and as we will discuss in the conclusions, this might even provide a beneficial new perspective for the development of anode materials for FIBs.

(3) Sc, Ti, V, Zr, Nb, Hf, and Ta also show a strong tendency to form carbides prior to the reduction of the metal fluoride. In contrast to the alkaline and alkaline earth metals, the corresponding carbides MC_x have values of $x \approx 1$, and the structures of the metal carbides are not related to the structure of graphite. This implies that at the interface to the carbon additive, a large amount of M species would have to be built up, accompanied by a reconstructive reorganization of C and M species for carbide formation. Thus, although the formation of MC_x is energetically favoured, overpotentials arising from this redistribution might reduce the likelihood of carbide formation. Nevertheless, once metal carbide clusters form, they are likely to show reduced reversibility for reconverting, which is related to the high melting temperatures of these carbide materials.[21] One must also consider that the metals M have high melting temperatures themselves, which could severely impede the conversion process between the metal and the metal fluoride as well. This would likely explain why these metal fluorides have not been reported to be used as anode materials so far, though their potentials and

capacities would reasonably justify their experimental investigation.

(4) Cr, Mn, Fe, Co, Ni, Mo, W, and Re have values of $\Delta U \approx 0$. Therefore, carbide formation vs. metal formation will strongly depend on overpotentials ϕ/ϕ' for the different reactions. Since all these metals have high melting potentials and the corresponding metal carbides MC_x have values of $x \ll 1$, both processes become unfavourable, and these metals are unlikely to be reasonably exploited as anode or cathode materials within conversion-type reactions in the authors' opinion.

(5) The different lanthanides LnC_x deserve special attention since many of their corresponding metal fluorides have been considered as solid electrolytes for FIBs. Remarkably, all lanthanides appear to energetically favor carbide formation over metal formation within a FIB. However, the values of x considerably fluctuate for the different lanthanides, with $x \approx 1$ or $x \gg 1$. Only Eu and Yb seem to favour the formation of graphite intercalation compounds $x \gg 1$ from an energetic viewpoint. However, because carbide formation appears to be generally favourable for lanthanides, one can imagine that these metals would have a strong tendency to form M–C adducts to non-graphite-like regions of carbon additives, which would be energetically susceptible to the formation of lanthanide carbides. Therefore, we assume that the carbide reaction might indeed prove to be a limiting factor for the use of LnF_y-based electrolytes[22] at the anode sides and that their usability with low-potential anodes must be conceptually reconsidered.

Conclusions

In this work, we have shown that carbide formation has the potential to be a significant side reaction for metal fluoride MF_y conversion-based electrodes within fluoride-ion batteries (FIBs). This is most severe in combination with electropositive metals such as alkali, alkaline earth, lanthanides and early 3d/4d/5d transition metals but is an unlikely process with anodes such as Sn, Pb, Zn. Although carbide formation would be favoured for all these metals, we emphasize that kinetic barriers might facilitate this process most strongly for carbon-rich carbides MC_x with $x \gg 1$, whose structures can be derived from the layered graphite arrangement. However, the complexity of carbon additives, which can also contain nongraphitic regions with higher energies, might render carbon reduction with metal adducts a possible scenario for metals that can form stable carbides and other metals as well. This reaction should be considered as a potential side reaction within anode materials for FIBs in the future and has not been considered in previous research so far.

Furthermore, we think that carbide formation, especially in the context of metal insertion into graphite, could in principle be exploited for designing anode materials for FIBs. This metal fluoride conversion in combination with metal insertion into graphite host lattices provides the opportunity for improving the cycling stability of conversion anodes, which is currently considered a key limitation for the development of functional FIBs. This result is reminiscent of previous work on cathode development for lithium-ion batteries, for example, by Reddy et al.[23] who used iron metal fluorides at the cathode side (from reacting Fe with carbon fluoride via ball milling) for fluoride storage in the conversion of LiF according to $LiF + Fe \rightarrow FeF_2 + 2\,Li^+ + 2\,e^-$.

Thus, the successful implementation of metals into carbon networks might provide the opportunity to create novel nanostructured anodes with improved reversibility. Although this would imply a reduction in the gravimetric capacity and a reduction of operation potential, this process could be a cheap alternative in combination with light alkaline earth metals, such as Ca^{2+} or Mg^{2+}[24] (e.g., $C_{grav,theo} = 860\ mAh\,g^{-1}$ for Mg/MgF_2 vs. $C_{grav,theo} = 399\ mAh\,g^{-1}$ for the hypothetical pair $MgC_6/MgF_2 + C_6$). Although the intercalation of carbon is not known for the naked metal cations, it can be supported by the addition of complexation agents and intercalation of the complex instead of the naked metal ion for M=Ca, Mg, Na.

We also think that potassium fluoride KF might deserve special attention for designing electrodes with high reversibility, especially within all solid-state FIBs. The potential for potassium insertion into carbon is at a potential similar to graphite materials used for lithium-ion batteries (see Figure 5). For $KF + 8\,C + e^- \rightarrow KC_8 + F^-$, the capacity would be at a reasonable value of $C_{grav.theo.} = 174\ mAh\,g^{-1}$. More remarkably, considering the molar volumes of the different reaction partners, the volume change would be as low as +/-2.5% for changing between the charged and discharged state. Additionally, potassium and carbon have a high abundance and would not represent a limiting factor for battery manufacturing.

Experimental Section

Our dataset is comprised of fluoride (MF_y) and carbide (MC_x) structures from the Materials Project[8] and was analysed using the Simulated Materials Ecosystem (Simmate)[25] and pymatgen.[26] The Materials Project database was initially screened to include all binary metal fluorides (522 structures). For compositions with more than one known phase, only the most stable phase was used to ensure that each composition was represented by a single entry (258 structures). The Materials Project database was re-screened for each M–F compound to identify M–C compounds (carbides). Like the M–F materials, some M–C compositions had more than one phase so only the most stable of these was used. This still allowed for multiple compositions of the same M–C system. Carbides were paired with the original fluoride such that all unique fluoride/carbide combinations (930) for element M were represented.

Unstable metal fluorides with a convex hull energy < 0.075 eV/atom were included to account for computational uncertainty. This excluded the most unstable fluorides, including subfluorides of various metals (e.g., Fe_3F), which are beyond any practical realization. The 0.075 eV/atom cutoff was chosen because systematic and random errors in DFT-derived formation energies sometimes calculate a stable compound to be unstable. These errors arise from electron self-interaction in localized electronic states and the correction techniques employed by Materials Project typically bring the errors within this 0.075 eV/atom range.[25–27] Some

elements only had carbide structures with hull energies close to or above the 0.075 eV/atom limit (e.g., Co_2C) but were still included in later analysis due to their interesting structural properties. For each fluoride/carbide pair, relevant properties like reduction potentials, hull stability, and space group were assembled and are presented in Table S1.

Supporting Information

Supporting Information is available online and includes: 1) A Dataset of all fluoride/carbide pairs obtained from screening of the Materials Project database. The $U(M/MF_y)$, $U(MC_x/MF_y+C)$, and $\Delta U(MC_x-M)$ columns were calculated using the formation enthalpies of each pair. 2) A comparison of $U(M/MF_y)_{vs.\ Li/LiF}$, $U(MC_x/MF_y+{}^{x}/_{60}\ C_{60})_{vs.\ Li/LiF}$, and the corresponding $\Delta U(MC_x-M)$ for the different combinations of stable MF_y with a low value of y and the thermodynamically most stable carbide MC_x. Actinides were not considered for the calculations since they do not show practical relevance. Furthermore, certain elements (Tc, Pm, Pb, Sb, Bi, Te, Po) did not contain any entries for their corresponding metal carbides. Furthermore, some elements form molecular carbides (H, N, O, S, Cl, Br, I) or do not form carbides at all (noble gases) and were thus not included.

Acknowledgements

S. C. Warren and O. Clemens acknowledge funding via the Staff Mobility Program between the states of North Carolina, USA, and Baden-Württemberg, Germany. O. Clemens acknowledges funding by the German Research Foundation (DFG) within CL551/2-1. Open Access funding enabled and organized by Projekt DEAL.

Conflict of Interests

There are no conflicts of interest to declare.

Data Availability Statement

The data that support the findings of this study are available from the corresponding author upon reasonable request.

Keywords: Fluoride-Ion Batteries · Conversion Electrodes · Carbide Formation · Database Screening · Hierarchical Search

[1] J. Xu, F. Lin, M. M. Doeff, W. Tong, *J. Mater. Chem. A* **2017**, *5*, 874–901.
[2] a) M. Anji Reddy, M. Fichtner, *J. Mater. Chem.* **2011**, *21*, 17059–17062; b) M. A. Nowroozi, I. Mohammad, P. Molaiyan, K. Wissel, A. R. Munnangi, O. Clemens, *J. Mater. Chem. A* **2021**, *9*, 5980–6012.
[3] R. W. Bonne, J. Schoonman, *J. Electrochem. Soc.* **1977**, *124*, 28–35.
[4] a) V. K. Davis, C. M. Bates, K. Omichi, B. M. Savoie, N. Momcilovic, Q. Xu, W. J. Wolf, M. A. Webb, K. J. Billings, N. H. Chou, S. Alayoglu, R. K. McKenney, I. M. Darolles, N. G. Nair, A. Hightower, D. Rosenberg, M. Ahmed, C. J. Brooks, T. F. Miller, 3rd, R. H. Grubbs, S. C. Jones, *Science* **2018**, *362*, 1144–1148; b) F. Gschwind, Z. Zao-Karger, M. Fichtner, *J. Mater. Chem. A* **2014**, *2*, 1214–1218; c) M. Kawasaki, K.-I. Morigaki, G. Kano, H. Nakamoto, R. Takekawa, J. Kawamura, T. Minato, T. Abe, Z. Ogumi, *J. Electrochem. Soc.* **2021**, *168*, 010529; d) K.-i. Okazaki, Y. Uchimoto, T. Abe, Z. Ogumi, *ACS Energy Lett.* **2017**, *2*, 1460–1464; e) T. Yamamoto, K. Matsumoto, R. Hagiwara, T. Nohira, *ACS Appl. Energ. Mater.* **2019**, *2*, 6153–6157.
[5] a) S. T. Hartman, R. Mishra, *J. Mater. Chem. A* **2020**, *8*, 24469–24476; b) W. Zaheer, J. L. Andrews, A. Parija, F. P. Hyler, C. Jaye, C. Weiland, Y. S. Yu, D. A. Shapiro, D. A. Fischer, J. H. Guo, J. M. Velazquez, S. Banerjee, *ACS Energy Lett.* **2020**, *5*, 2520–2526; c) M. A. Nowroozi, K. Wissel, J. Rohrer, A. R. Munnangi, O. Clemens, *Chem. Mater.* **2017**, *29*, 3441–3453; d) M. A. Nowroozi, B. de Laune, O. Clemens, *ChemistryOpen* **2018**, *7*, 617–623; e) M. A. Nowroozi, S. Ivlev, J. Rohrer, O. Clemens, *J. Mater. Chem. A* **2018**, *6*, 4658–4669; f) M. A. Nowroozi, K. Wissel, M. Donzelli, N. Hosseinpourkahvaz, S. Plana-Ruiz, U. Kolb, R. Schoch, M. Bauer, A. M. Malik, J. Rohrer, S. Ivlev, F. Kraus, O. Clemens, *Commun. Mater.* **2020**, *1*, 27.
[6] K. Wissel, R. Schoch, T. Vogel, M. Donzelli, G. Matveeva, U. Kolb, M. Bauer, P. R. Slater, O. Clemens, *Chem. Mater.* **2021**, *33*, 499–512.
[7] a) K. Wissel, J. Heldt, P. B. Groszewicz, S. Dasgupta, H. Breitzke, M. Donzelli, A. I. Waidha, A. D. Fortes, J. Rohrer, P. R. Slater, G. Buntkowsky, O. Clemens, *Inorg. Chem.* **2018**, *57*, 6549–6560; b) K. Wissel, A. M. Malik, S. Vasala, S. Plana-Ruiz, U. Kolb, P. R. Slater, I. da Silva, L. Alff, J. Rohrer, O. Clemens, *Chem. Mater.* **2020**, *32*, 3160–3179.
[8] A. Jain, S. P. Ong, G. Hautier, W. Chen, W. D. Richards, S. Dacek, S. Cholia, D. Gunter, D. Skinner, G. Ceder, K. A. Persson, *APL Mater.* **2013**, *1*.
[9] M. Inagaki, F. Kang, *Materials Science and Engineering of Carbon: Fundamentals*, Elsevier, Oxford, UK, **2014**.
[10] G. K. Wertheim, P. M. T. M. Van Attekum, S. Basu, *Solid State Commun.* **1980**, *33*, 1127–1130.
[11] O. Dolotko, A. Senyshyn, M. J. Mühlbauer, K. Nikolowski, H. Ehrenberg, *J. Power Sources* **2014**, *255*, 197–203.
[12] P. Lagrange, D. Guerard, A. Herold, *Ann. Chim.* **1978**, *3*, 143–159.
[13] M. E. Makrini, D. Guérard, P. Lagrange, A. Hérold, *Carbon* **1980**, *18*, 203–209.
[14] R. E. Gebelt, H. A. Eick, *Inorg. Chem.* **2002**, *3*, 335–337.
[15] A. L. Giorgi, E. G. Szklarz, N. H. Krikorian, M. C. Krupka, *J. Less-Common Met.* **1970**, *22*, 131–135.
[16] I. G. Wood, L. Vočadlo, K. S. Knight, D. P. Dobson, W. G. Marshall, G. D. Price, J. Brodholt, *J. Appl. Crystallogr.* **2004**, *37*, 82–90.
[17] a) J. Bernstein, E. Armon, E. Zemel, E. Kolodney, *J. Phys. Chem. A* **2013**, *117*, 11856–11865; b) J. E. Reddic, M. A. Duncan, *Chem. Phys. Lett.* **1997**, *264*, 157–162; c) B. W. Ticknor, B. Bandyopadhyay, M. A. Duncan, *J. Phys. Chem. A* **2008**, *112*, 12355–12366.
[18] M. A. Nowroozi, O. Clemens, *ACS Appl. Energ. Mater.* **2018**, *1*, 6626–6637.
[19] a) I. Mohammad, J. Chable, R. Witter, M. Fichtner, M. A. Reddy, *ACS Appl. Mater. Interfaces* **2018**, *10*, 17249–17256; b) I. Mohammad, R. Witter, M. Fichtner, M. Anji Reddy, *ACS Appl. Energ. Mater.* **2018**, *1*, 4766–4775.
[20] a) O. Clemens, C. Rongeat, M. A. Reddy, A. Giehr, M. Fichtner, H. Hahn, *Dalton Trans.* **2014**, *43*, 15771–15778; b) C. Rongeat, M. Anji Reddy, T. Diemant, R. J. Behm, M. Fichtner, *J. Mater. Chem. A* **2014**, *2*, 20861–20872; c) C. Rongeat, M. Anji Reddy, R. Witter, M. Fichtner, *ACS Appl. Mater. Interfaces* **2014**, *6*, 2103–2110.
[21] A. F. Holleman, N. Wiberg, *Lehrbuch der Anorganischen Chemie, 101. Auflage*, deGruyter, Berlin, **1995**.
[22] a) C. Rongeat, M. A. Reddy, R. Witter, M. Fichtner, *J. Phys. Chem. C* **2013**, *117*, 4943–4950; b) C. Rongeat, M. A. Reddy, R. Witter, M. Fichtner, *ACS Appl. Mater. Interfaces* **2014**, *6*, 2103–2110; c) A. Duvel, J. Bednarcik, V. Sepelak, P. Heitjans, *J. Phys. Chem. C* **2014**, *118*, 7117–7129; d) J. Chable, B. Dieudonne, M. Body, C. Legein, M. P. Crosnier-Lopez, C. Galven, F. Mauvy, E. Durand, S. Fourcade, D. Sheptyakov, M. Leblanc, V. Maisonneuve, A. Demourgues, *Dalton Trans.* **2015**, *44*, 19625–19635; e) B. Dieudonné, J. Chable, F. Mauvy, S. Fourcade, E. Durand, E. Lebraud, M. Leblanc, C. Legein, M. Body, V. Maisonneuve, A. Demourgues, *J. Phys. Chem. C* **2015**, *119*, 25170–25179; f) H. Bhatia, D. T. Thieu, A. H. Pohl, V. S. K. Chakravadhanula, M. H. Fawey, C. Kubel, M. Fichtner, *ACS Appl. Mater. Interfaces* **2017**, *9*, 23707–23715; g) J. Chable, A. G. Martin, A. Bourdin, M. Body, C. Legein, A. Jouanneaux, M. P. Crosnier-Lopez, C. Galven, B. Dieudonné, M. Leblanc, A. Demourgues, V. Maisonneuve, *J. Alloys Compd.* **2017**, *692*, 980–988; h) B. Dieudonne, J. Chable, M. Body, C. Legein, E. Durand, F. Mauvy, S. Fourcade, M. Leblanc, V. Maisonneuve, A. Demourgues, *Dalton Trans.* **2017**, *46*, 3761–3769.
[23] M. A. Reddy, B. Breitung, V. S. K. Chakravadhanula, C. Wall, M. Engel, C. Kübel, A. K. Powell, H. Hahn, M. Fichtner, *Adv. Energy Mater.* **2013**, *3*, 308–313.

[24] a) D.-M. Kim, S. C. Jung, S. Ha, Y. Kim, Y. Park, J. H. Ryu, Y.-K. Han, K. T. Lee, *Chem. Mater.* **2018**, *30*, 3199–3203; b) S. J. Richard Prabakar, A. B. Ikhe, W. B. Park, K. C. Chung, H. Park, K. J. Kim, D. Ahn, J. S. Kwak, K. S. Sohn, M. Pyo, *Adv. Sci. (Weinheim, Ger.)* **2019**, *6*, 1902129.
[25] J. D. Sundberg, S. S. Benjamin, L. M. McRae, S. C. Warren, *J. Open Source Softw.* **2022**, *7*.
[26] S. P. Ong, W. D. Richards, A. Jain, G. Hautier, M. Kocher, S. Cholia, D. Gunter, V. L. Chevrier, K. A. Persson, G. Ceder, *Comput. Mater. Sci.* **2013**, *68*, 314–319.
[27] a) A. Wang, R. Kingsbury, M. McDermott, M. Horton, A. Jain, S. P. Ong, S. Dwaraknath, K. A. Persson, *Sci. Rep.* **2021**, *11*, 15496; b) A. Jain, G. Hautier, S. P. Ong, C. J. Moore, C. C. Fischer, K. A. Persson, G. Ceder, *Phys. Rev. B* **2011**, *84*; c) M. K. Horton, S. Dwaraknath, K. A. Persson, *Nat. Comput. Sci.* **2021**, *1*, 3–5.

Manuscript received: April 5, 2023
Revised manuscript received: May 11, 2023
Accepted manuscript online: May 12, 2023
Version of record online: July 17, 2023